sustainability

MDPI

Article

Minimum Velocity of Impingement Fluidization for Parachute-Shaped Vegetables

Dariusz Góral [1,*], Tomasz Guz [2] and Urszula Pankiewicz [3]

[1] Department of Biological Bases of Food and Feed Technologies, Faculty of Production Engineering, University of Life Sciences in Lublin, 20-612 Lublin, Poland
[2] Department of Engineering and Food Machines, Faculty of Production Engineering, University of Life Sciences in Lublin, 20-612 Lublin, Poland; tomasz.guz@up.lublin.pl
[3] Department of Analysis and Food Quality Assessment, Faculty of Food Science and Biotechnology, University of Life Sciences in Lublin, 20-704 Lublin, Poland; urszula.pankiewicz@up.lublin.pl
* Correspondence: dariusz.goral@up.lublin.pl; Tel.: +48-815319738

Abstract: Accurate calculation of the minimum fluidization velocity makes it possible to reduce raw material losses due to the use of excessively high or excessively low air velocities. This is particularly true for impingement fluidization, which is little studied, especially when treating parachute-shaped raw material. This paper focused on determining the drag coefficient for cauliflower florets, mushrooms, and broccoli. Analysis of the critical particle lift velocity showed that the lowest value of the drag coefficient was found for mushrooms (0.9). The parachute-shaped vegetables analyzed had a large scatter of drag coefficient values associated with their specific shape (standard deviation: mushrooms 0.10 broccoli 0.14, and for cauliflower 0.15). The measured mean values of the minimum fluidization velocity of the tested vegetables in the impingement fluidization method ranged from 6.9 $m \cdot s^{-1}$ to 10.97 $m \cdot s^{-1}$. Application of the procedure recommended by Shilton and Narajan for calculating the minimum fluidization velocity on the basis of the shape coefficient ε resulted in large discrepancies between the calculated and experimental values (from 2.4 $m \cdot s^{-1}$ to 3.8 $m \cdot s^{-1}$).

Keywords: parachute-shaped vegetable; drag coefficient; minimum velocity of fluidization; impingement fluidization

Citation: Góral, D.; Guz, T.; Pankiewicz, U. Minimum Velocity of Impingement Fluidization for Parachute-Shaped Vegetables. *Sustainability* **2022**, *14*, 4257. https://doi.org/10.3390/su14074257

Academic Editors: Roland Jochem and Marcel Randermann

Received: 18 March 2022
Accepted: 28 March 2022
Published: 3 April 2022

1. Introduction

Gas-solid fluidization, an operation that involves passing gas through a bed of solid particles to suspend the particles in a fluid-like state, has a wide range of applications in the food industry, including fruit and vegetable freezing, drying, biomass gasification, and grain equilibration. The growing popularity of fluidized beds is due to well-known advantages such as excellent heat and mass transfer and ease of operation, among others [1].

Fluidized bed heat treatment of raw materials with jet impingements is in many cases a new processing method for the food industry. Impingement fluidization is a specific type of the food freezing fluidization process. The method is based on the impingement phenomenon that causes fluidized boiling in the product bed [2]. In this method, after reaching the minimum velocity of fluidization, the buoyant force exceeds the gravitational force of the product, which is transported toward the top of the fountain. Then, due to mutual interactions between adjacent bed particles, individual elements are lifted to the edge of the fountain top and transported to the zone of lower air pressure or the air flow coming out of the nozzle [3–5]. This causes the particles to fall to the bottom of the working chamber of the apparatus and start a new process cycle (Figure 1).

On the other hand, an excessively low fluidization speed will result in inadequate product quality. The raw material will be under-dried or not fully frozen. This, in turn, leads to high production losses. In industrial practice, the determination of the minimum fluidization speed is carried out experimentally. As a result, part of the raw material is

wasted, and energy consumption and production costs increase. The minimum fluidization velocity is considered to be an essential parameter in the successful fluidized bed characterization [6]. This velocity depends on the particle diameter and bed porosity, among other factors [7]. There are many formulas for calculating the minimum fluidization velocity [8–11]. However, they have been developed for industries other than food production, so they do not take into account such properties of agricultural and food products as shape irregularity or adhesion forces. In practice, most solutions to this problem are derived from Ergun's Equation (1) [12].

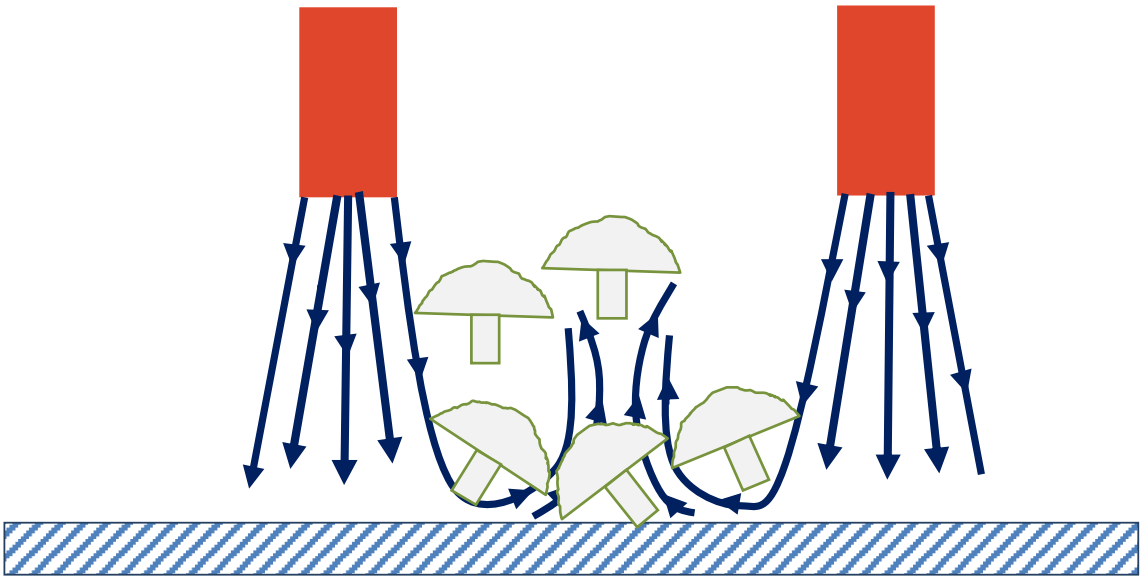

Figure 1. Motion of bed elements in impingement fluidization conditions.

$$\frac{\Delta P}{L} = 150\frac{(1-\varepsilon)^2}{\varepsilon^3}\frac{v\mu}{d^2} + 1.75\frac{1-\varepsilon}{\varepsilon^3}\frac{v^2\rho}{d} \quad (1)$$

The effect of shape on particle behavior during fluidization treatments is relatively unknown and not easily analyzed in real conditions [13]. A sphere can be easily and unambiguously characterized by its diameter, and a cube can be defined by the length of its side. In the case of food industry raw materials, there is a wide range of particles with irregular shapes that are difficult to define [14,15]. Sphericity f is one of the most commonly used parameters characterizing the shape of a particle. It is the ratio of the area of a sphere with a diameter identical to that of the particle to the area of the particle [16]. For non-spherical particles, sphericity values are in the range $0 < f < 1$.

Thompson and Clark [14] replaced the concept of sphericity with a new aspect ratio E, which is determined from the ratio of the drag coefficient for an irregular particle to the drag coefficient for a sphere [17].

$$\mathrm{E} = \frac{C_{DA}}{C_{DS}} \quad (2)$$

The drag coefficient depends on the shape of the particle and its position during motion. The size of the drag coefficient in turbulent flow is strongly influenced by the particle shape. The theoretical determination of the shape factor for parachute-shaped products seems to be particularly problematic. The difficulty in determining the shape of the product translates into the ability to determine the minimum fluidization velocity. Shilton and Niranjan [18] proposed the following procedure to determine the minimum fluidization velocity for non-spherical food particles:

assumption of the v value and calculation of the Reynolds number,
determination of particle sphericity,
calculation of ε from

$$\varepsilon = 0.42 f^{0.376} \quad (3)$$

estimation of friction factor
calculation of the minimum velocity of fluidization from the Equation (1).

There are 1946 papers on minimum fluidization velocity in the Scopus database. Of these papers, only 19 are concerned with determining the fluidization velocity of food. However, theoretical calculations for impingement fluidization are lacking. Due to the variety of product shapes and sizes, choosing the right equation to determine the minimum fluidization speed of food products is not easy, despite the widespread use of classical fluidization in the food industry. In particular, there is a lack of solutions for impact fluidization and considering products with a large bearing surface. Therefore, the aim of this work was to determine the drag coefficient for parachute-shaped products and to apply this coefficient in an existing analytical solution for determining the minimum fluidization velocity. The well-known and frequently used solution given by Shilton and Niranjan [18] was used for this purpose. This should facilitate the design of processes using impact fluidization and affect energy savings and loss reduction in the food industry.

2. Materials and Methods

2.1. Materials

The research material consisted of rosettes of Malaga cv. Cauliflower (water content 90%, density 1005 kg·m^{-3}), Polish button mushrooms (*Agaricus bisporus*) (water content 91%, density 760 kg·m^{-3}), and rosettes of Naxos cv. Broccoli (water content 85%, density 980 kg·m^{-3}). Before the analyses, the cauliflower and broccoli leaves were discarded, the vegetables were washed, the cauliflowers were divided into smaller rosettes with a ca. 35-mm diameter and 20-mm stalks, and the broccoli were divided into rosettes with a ca. 50-mm diameter and 20-mm stalks. Mushrooms with a cap approximately 40–60 mm in diameter and a 10–20 mm long stalk were selected for analysis. Next, the vegetables were rinsed and dried. The size distribution of the measured diameters is shown in the Figure 2.

The raw material prepared for the analyses was undamaged and had no signs of diseases.

2.2. Volume and Density

The volume and density of the samples were determined with the pycnometric method [19]. The dry matter content of the raw material was determined with the oven-drying method (at 135 °C for 2 h) [20].

2.3. Surface of the Cross-Sectional Area

The surface of the cross-sectional area (projected area) was determined using the indirect method. It consisted of taking a 1:1-scale black-and-white photograph of a raw material particle placed on a uniformly white background (Figure 3).

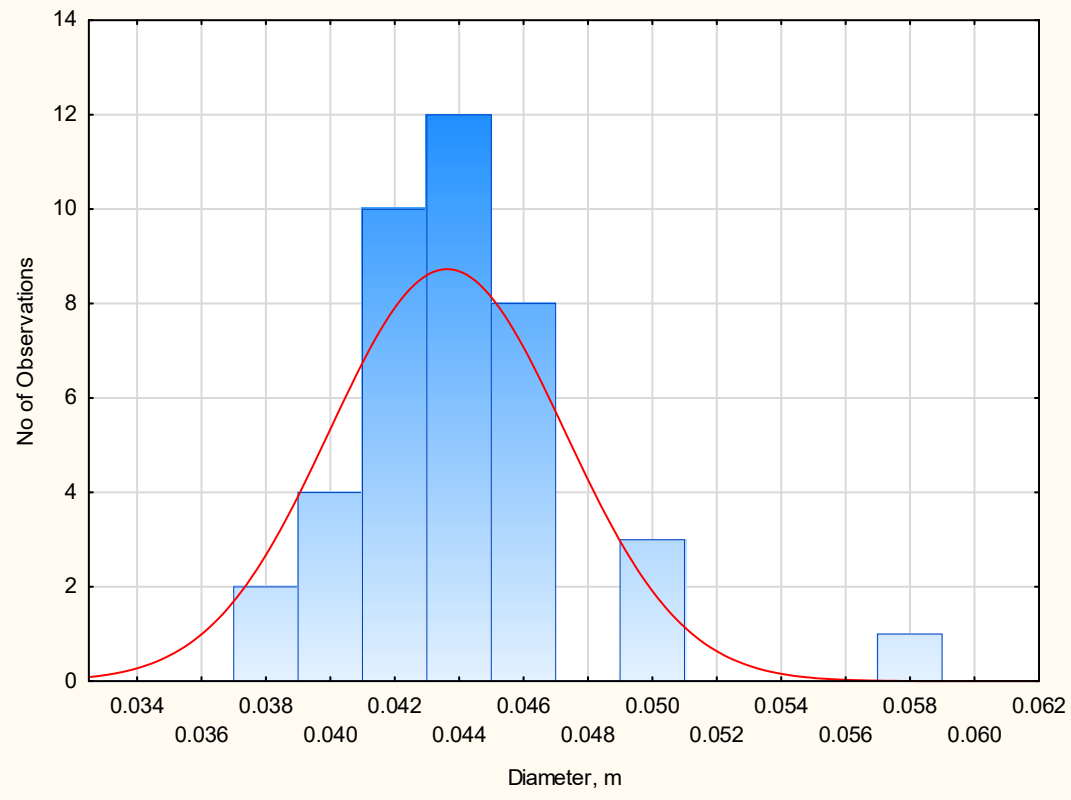

(**a**)

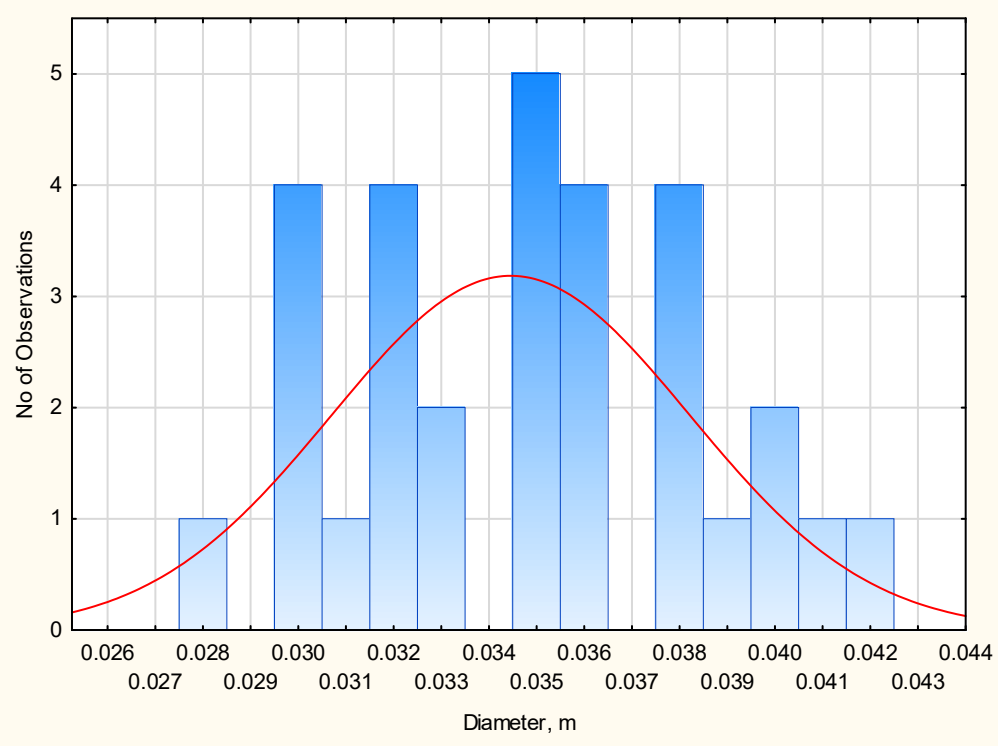

(**b**)

Figure 2. *Cont*.

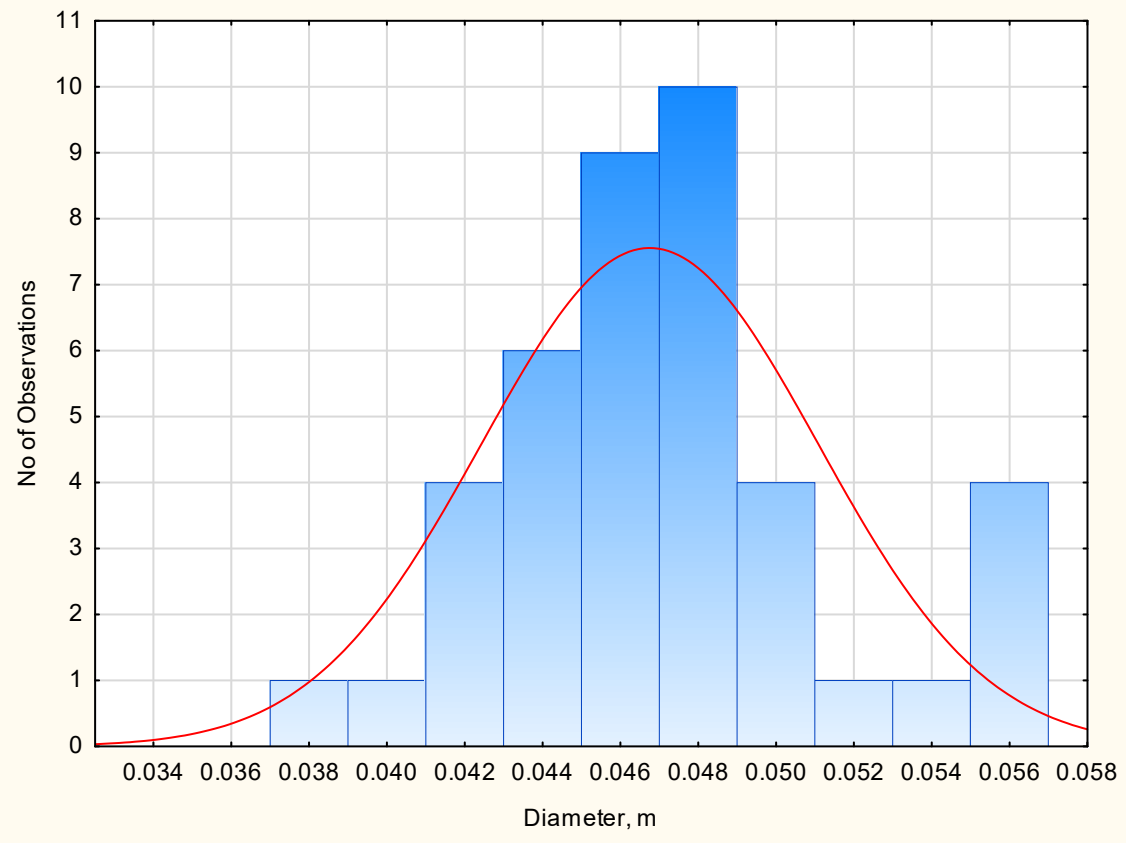

(**c**)

Figure 2. Size distribution of diameters: (**a**) Polish button mushrooms, (**b**) rosettes of cauliflower, and (**c**) rosettes of broccoli.

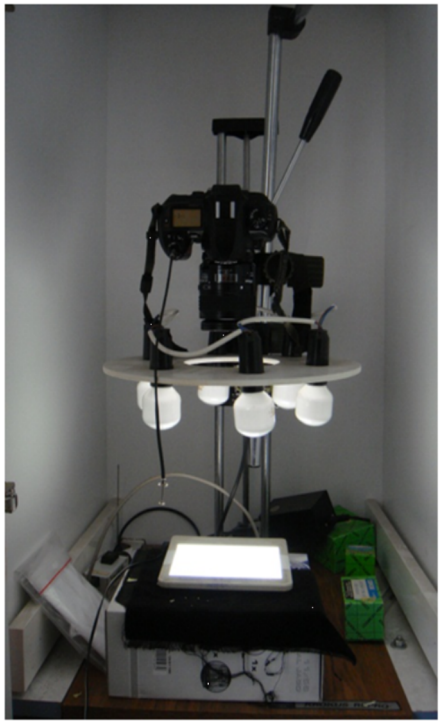

Figure 3. Test bench for determination of the projected area of the raw material.

Next, the percentage of image blackening was determined by reading the histogram. Given the surface area of the background, the blackened surface was calculated.

2.4. Critical Velocity

Critical velocity v_k was determined on a test bench consisting of a high-pressure fan (Nyborg–Mawent WP–20/1.5) with a capacity of 0.6 $m^3 \cdot s^{-1}$ at 2600 Pa, a refrigeration unit, and a Plexiglas pipe of 100 mm diameter and 3.5 mm wall thickness. The infinitely variable adjustment of the motor velocity was facilitated by a current frequency converter. At the bottom of the tube was a wheel to force a uniform airflow. Particle placement in the space was facilitated by a separator assembly consisting of a tube and the wheel. The airflow velocity and dynamic pressure were measured (KIMO Anemo—Manometer MP 120) using a Pitot tube of 3 mm diameter at the equilibrium point of the placed product particle at a height of a = 1000 mm (Figure 4) [21].

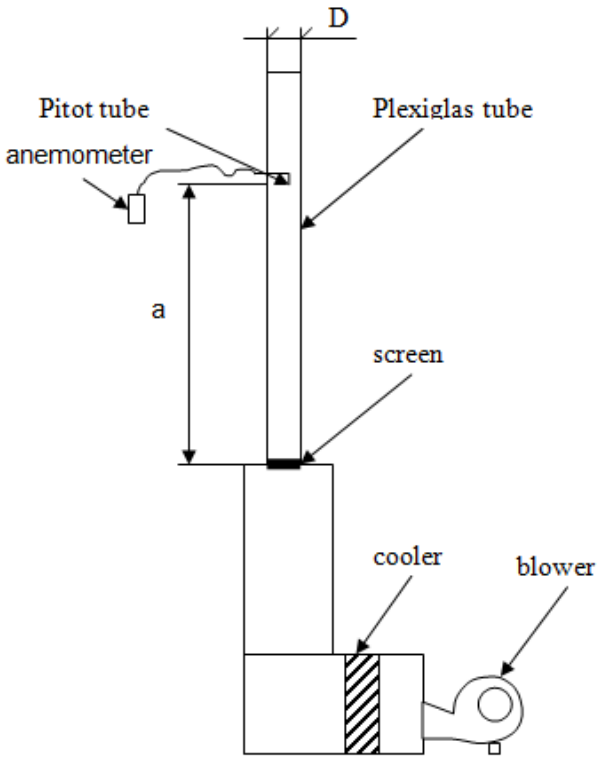

Figure 4. Test bench for determination of critical velocity v_k.

2.5. Calculation of Minimum Velocity of Fluidization

The minimum velocity of fluidization was determined using a modified procedure proposed by Shilton and Niranjan [18]. The sphericity coefficient f was replaced by the shape factor E.

2.6. Measurement of the Minimum Fluidization Velocity under Real Conditions during Impingement Fluidization

To compare the calculated values with the actual values, the minimum velocity of fluidization was measured. The experimental tests were carried out in a laboratory device equipped with a head consisting of a sieve bottom with dimensions of 0.41 × 0.36 × 0.018 m and 0.37-m-long nozzles placed in the bottom. The diameter of the nozzles was 20 mm. The airflow velocity was steplessly controlled by a current frequency transducer. A single layer of material was placed at the bottom of the working chamber. The velocity of the air jet rebound from the working chamber bottom was measured using an L-type Pitot probe connected to an anemometer (KIMO MP-120). Measurements were made at a con-

stant vertical distance of 70 mm between the tip of the Pitot probe and the bottom of the working chamber. The value measured during bed boiling was taken as the minimum fluidization velocity.

3. Results and Discussion

Many empirical factors have been proposed to describe non-spherical particles and correlate their flow behavior. An empirical description of the particle shape is obtained by determining two characteristic parameters (volume, surface area, projected area, projected perimeter) [22]. The photographic method produced 2D images of the materials (Figure 5). These images were used to determine the projected area of the vegetables. The surface area of the mushrooms deviated only slightly from the area of a circle with a diameter equal to the average diameter of the cap (on average by 3.92%).

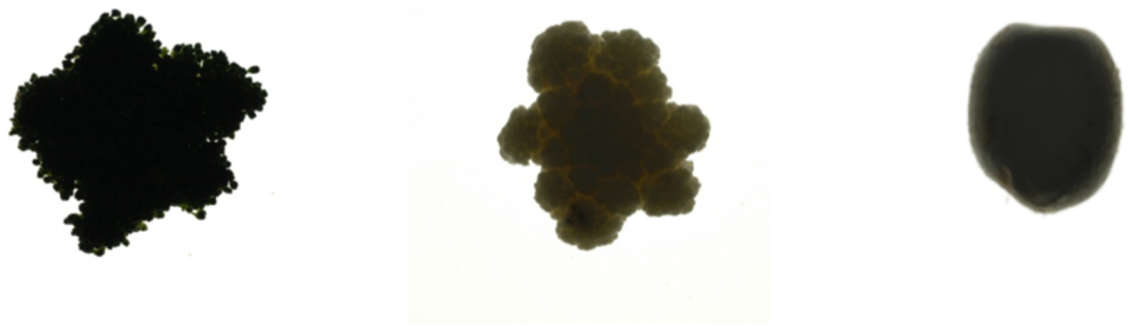

(**a**) (**b**) (**c**)

Figure 5. Examples of images used for determination of the projected area of the analyzed vegetables: (**a**) broccoli, (**b**) cauliflower, (**c**) mushroom.

In contrast, the projected area of the cauliflower and broccoli differed substantially from the equivalent area of a circle (by 34% and 23%, respectively).

The measured projected areas were characterized by a large dispersion of values and, simultaneously, similar values of mean diameters (Table 1).

Table 1. Mean values of the projected area and critical velocity of the analyzed vegetables.

	Mushroom		**Broccoli**		**Cauliflower**	
	Projected Area m^2	**Terminal Velocity m s^{-1}**	**Projected Area m^2**	**Terminal Velocity m s^{-1}**	**Projected Area m^2**	**Terminal Velocity m s^{-1}**
Average	0.001504	11.98723	0.00173	20.5512	0.005113	21.30667
Standard error	4.23×10^{-5}	0.155737	5.06×10^{-5}	0.200311	6.79×10^{-5}	0.24987
Median	0.00152	11.83216	0.001661	20.37155	0.005134	21.15
Standard deviation	0.000267	0.972577	0.000324	1.266879	0.000372	1.368597
Variance	7.15×10^{-8}	0.945906	1.05×10^{-7}	1.604981	1.38×10^{-7}	1.873057
Range	0.001566	3.904436	0.001387	5.040257	0.001432	5.1
Minimum	0.001075	10	0.001075	17.98147	0.004445	18.7
Maximum	0.002641	13.90444	0.002462	23.02173	0.005878	23.8

Knowledge of the critical transport velocity is necessary, among other things, to determine the maximum flow velocity of the fluidization medium above which the bed particles will be ejected [18]. Analysis of the critical transport velocity showed the lowest values of this parameter for mushrooms. In contrast, the mean values of the critical transport velocity for broccoli and cauliflower rosettes were similar (20 and 21 m·s^{-1}) and almost twice as high as for mushrooms. This was mainly related to the different densities of these products.

Thompson and Clark [14] reported that determination of the surface area of irregularly shaped particles is difficult, so they questioned the suitability of the sphericity coefficient f which is included in the Ergun equation. It seems that the difficulty in determining sphericity for parachute-shaped products can be overcome by using the drag coefficient. The value of drag coefficient for a single particle is determined by the balance between the mass of the particle, the air buoyancy force, and the drag coefficient [18]. The aerodynamic drag force is given by the formula [23]

$$F_{DA} = \frac{C_{DA} A \rho v_r^2}{2} \tag{4}$$

In the event that the force of gravity balances with the force of aerodynamic resistance, the particle is suspended in the air stream and there is no inertia force due to the lack of accelerations. Hence, drag coefficient can be calculated from the following relationship [23]:

$$C_{DA} = \frac{2mg}{A \rho v_k^2} \tag{5}$$

Figure 6 shows the relationship between the drag coefficient and the Reynolds number determined for the mushrooms.

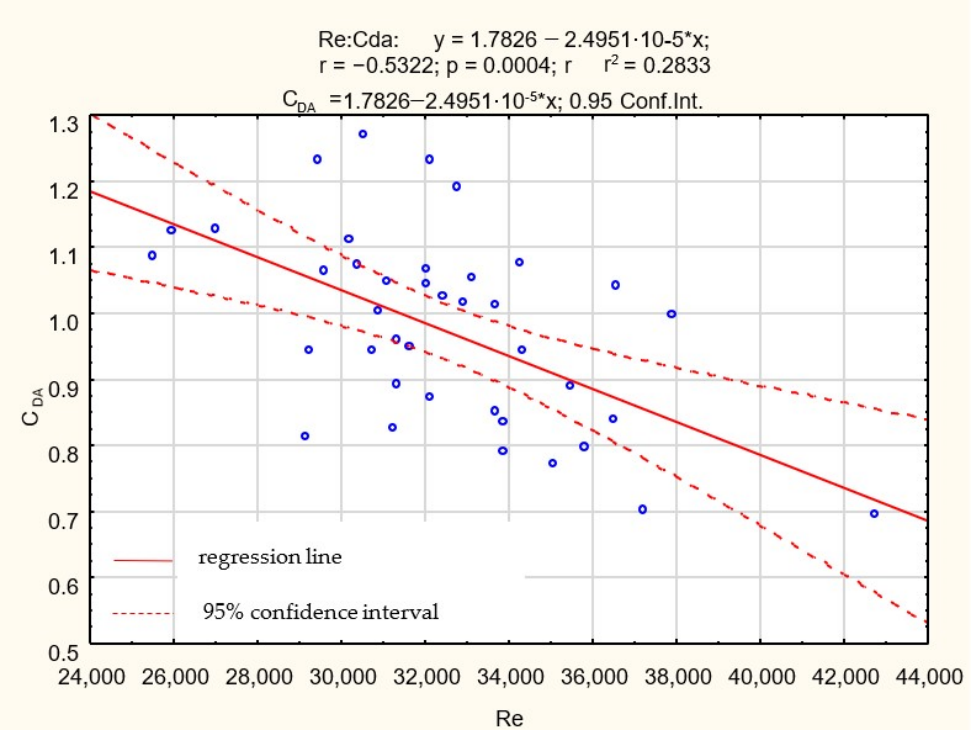

Figure 6. Dependence of the drag coefficient C_{DA} on the Reynolds number Re in the case of mushrooms.

Since the shape of the cap largely resembled a parachute canopy, high values of this coefficient were expected. The highest value of the drag coefficient was 1.2. Simultaneously, a very large dispersion of these values (from 1.2 to 0.7) was noted. The low values of the drag coefficient in some mushrooms were related to the presence of the veil enclosing the cap; hence, the mushrooms had the shape of a closed hemisphere rather than a parachute canopy.

The next products analyzed in this study were Broccoli florets (Figure 7). There was a large dispersion of the drag coefficient values in this case as well.

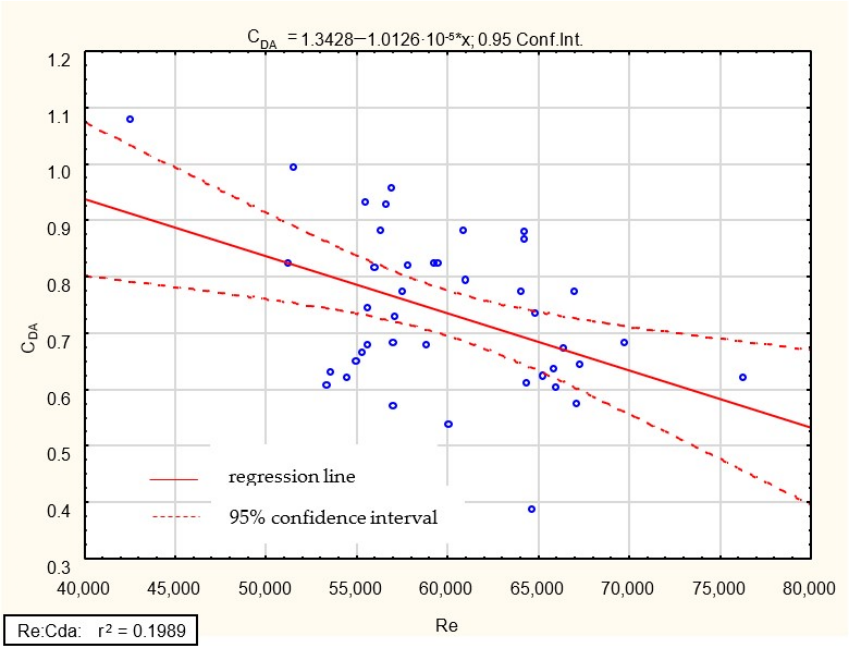

Figure 7. Changes in the drag coefficient C_{DA} depending on the Reynolds number Re in the case of broccoli rosettes.

The dispersion was caused by the structure of the rosettes. Broccoli florets with a compact structure and often inwardly curved edges were shaped more like a sphere than a parachute, hence the low drag coefficient values.

Cauliflower florets were the other vegetables tested with a parachute-like shape. Analysis of this raw material revealed lower drag coefficient values despite the similar morphology of cauliflower and broccoli florets (Figure 8).

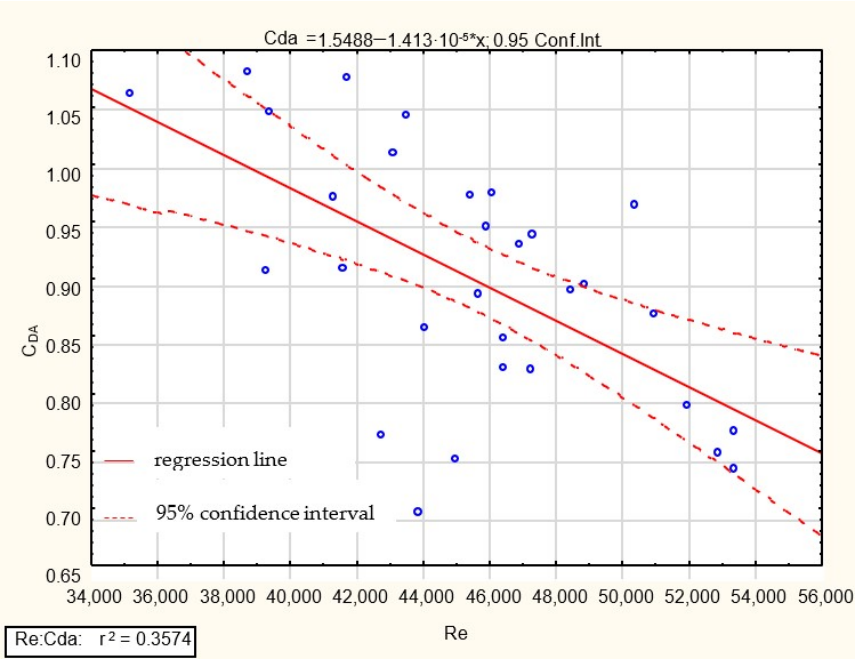

Figure 8. Dependence of the drag coefficient C_{DA} on the Reynolds number Re in the case of cauliflower rosettes.

The drag coefficient depends not only on the shape, but also on the size and inclination of the object as well as the conditions of airflow through the object. It seems that the differences in the values of this coefficient between the cauliflower and broccoli florets are due to the more compact structure and more spherical shape of the cauliflower inflorescence.

The next stage of the research consisted of measuring and calculating the minimum velocity of the fluidization onset in the impingement type fluidization device used to process the raw material. Due to specific nature of the process and the type of material processed, a single-layer bed was used (Figure 9).

Figure 9. Boiling bed of a single layer of broccoli rosettes subjected to the impingement fluidization treatment.

The equations used in this work were applied to a bulk of particles with size lower that 1 millimeter (Geldart diagram). However, the use of this classification for food is not justified. Moreover, the Ergun equation is the widely accepted model for determining the minimum fluidization velocity of a fluid to fluidize any material [24]. Additionally, the authors [18] recommend the cited method for estimating of minimum fluidization velocity for non-spherical food particles. The Ergun's equation is of course used for packed beds. However, it is the basis for deriving various formulas for calculating the minimum fluidization velocity. It is also the basis of the method proposed by Shilton and Niranjan [18], which was used for calculations in this paper. For non-spherical particles, drag coefficient was used instead of sphericity and equivalent diameter.

Broccoli and cauliflower rosettes were characterized by the highest value of the minimum fluidization velocity in the impingement fluidization freezing (9 $m \cdot s^{-1}$ and 11 $m \cdot s^{-1}$, respectively). As expected, the lowest minimum fluidization velocity was noted during mushroom processing (7 $m \cdot s^{-1}$). This depended largely on particle mass and to a lesser extent on particle shape. The procedure proposed by Shilton and Niranjan [18] was used to determine the minimum velocity of the fluidization onset. The ratio of the particle drag coefficient to the sphere drag coefficient was taken as the shape factor. The calculated minimum fluidization velocity values ranged from 2.4 $m \cdot s^{-1}$ for the mushrooms to 3.8 $m \cdot s^{-1}$ for the cauliflower and broccoli (Table 2). The *t*-test was performed to compare means of samples and an F-test to compare variances. Since the *p*-value for the *t*-test was

less than 0.05, there was a statistically significant difference between the means at the 5% significance level.

Table 2. Experimental results of minimum velocity fluidization.

	Minimum Fluidization Velocity, $m \cdot s^{-1}$	Average, $m \cdot s^{-1}$	Standard Deviation, $m \cdot s^{-1}$	Confidence Level 95%, $m \cdot s^{-1}$
mushroom	6.2 7.5 7.0	6.9	0.66	1.63
broccoli	8.9 8.7 9.5	9.03	0.42	1.03
cauliflower	11.1 11.1 10.7	10.97	0.23	0.57

Significant differences between calculated and experimentally obtained air velocity values were probably related to the peculiarities of the impingement fluidization phenomenon. In this method, a portion of the energy of the air stream exiting a single nozzle is dissipated by adjacent air streams. Therefore, a higher air velocity is required to induce the fluidization process.

4. Conclusions

Impingement fluidization is a method of raw material processing increasingly used in the food industry. This method is often used to support other methods such as microwave drying or coffee roasting. In spite of the fact that impingement fluidization has been known since the 90s of the 20th century [25], there are very few works concerning it. A particularly important process parameter is the minimum fluidization velocity. Knowledge of this parameter enables accurate design of the process and reduction of raw material and energy losses. The computational determination of the minimum fluidization velocity of regular shaped particles is basically solved. In many works, one can find formulas approximating the value of this parameter with high accuracy. In the case of irregularly shaped particles, analytical methods often yield results with a large error. In the food industry the most difficult particles to describe are those with a parachute shape. For fluidization, this shape strongly affects the minimum fluidization velocity. Therefore, the study conducted on the drag coefficient of this type of particles is important. In this paper, a novel photographic method was used to calculate the projected area of complex shaped vegetables. This made it possible to determine the exact bearing surface of the vegetables. Knowing this surface area, the terminal velocity was calculated. The parachute-shaped vegetables analyzed had a large scatter of terminal velocity values (mushrooms 11.99 ± 0.97 m/s, cauliflower 21.3 ± 1.37, and broccoli 20.55 ± 1.27) due to their different shapes. The minimum fluidization velocity can be calculated analytically in a number of ways. One of them is the procedure recommended by Shilton and Narayan [18]. Due to the difficulty in unambiguously determining the shape, the drag coefficient was used for the calculation. The results ranged from 2.4 $m \cdot s^{-1}$ for the mushrooms to 3.8 $m \cdot s^{-1}$ for the cauliflower and broccoli. The experiments conducted produced actual minimum velocities. The results were 9 $m \cdot s^{-1}$ and 11 $m \cdot s^{-1}$ for broccoli and cauliflower rosettes, respectively, and 7 $m \cdot s^{-1}$ for mushrooms. It was found that the application of the Shilton and Narajan procedure to the calculation of the minimum fluidization velocity results in values with a large discrepancy between the calculated and experimentally obtained values. Therefore, it seems necessary to develop a new procedure for calculating the minimum fluidization velocity that can be used to design the impingement fluidization treatment of parachute-shaped vegetables.

Author Contributions: Conceptualization, D.G.; methodology, D.G.; investigation, T.G.; writing—original draft preparation, D.G.; writing—review and editing, U.P. All authors have read and agreed to the published version of the manuscript.

Funding: This research received no external funding.

Institutional Review Board Statement: Not applicable.

Informed Consent Statement: Not applicable.

Data Availability Statement: Not applicable.

Conflicts of Interest: The funders had no role in the design of the study; in the collection, analyses, or interpretation of data; in the writing of the manuscript, or in the decision to publish the results.

Nomenclature

a	height: m (Figure 4)
A	projected area, m^2
C_D	drag coefficient
d	particle diameter, m
E	shape factor
F	drag force, N
f	sphericity
g	acceleration due to gravity, $m{\cdot}s^{-2}$
L	length of the bed, m
m	mass, kg, g
ΔP	pressure drop through the packed bed, Pa
V	particle volume, m^3
v_k	critical velocity, $m{\cdot}s^{-1}$
v	superficial fluid velocity, $m{\cdot}s^{-1}$
ε	bed voidage
μ	dynamic viscosity of air, Pa·s
ρ_f	density of air, $kg{\cdot}m^{-3}$
ρ_s	density of product, $kg{\cdot}m^{-3}$
x	particle size, m
Dimensionless numbers:Ar	Archimedes number, $Ar = \frac{gd^3\rho_f(\rho_s-\rho_f)}{\mu^2}$
Dimensionless numbers:Re	Reynolds number, $\mathrm{Re} = \frac{vd\rho}{\mu}$

References

1. Anantharaman, A.; Cocco, R.A.; Chew, J.W. Evaluation of correlations for minimum fluidization velocity (Umf) in gas-solid fluidization. *Powder Technol.* **2018**, *323*, 454–485. [CrossRef]
2. Cho, H.R.; Kim, S.Y.; Nam, J.S.; Cho, H.Y. Effects of air temperature on the physicochemical properties and flavor compounds of roasted red ginseng lateral roots in a jet impingement fluidized bed roaster. *LWT* **2021**, *146*, 111480. [CrossRef]
3. Góral, D.; Kluza, F.; Kozłowicz, K. Spouted Bed and Jet Impingement Fluidization in Food Industry. In *Heat Transfer—Models, Methods and Applications*; IntechOpen: London, UK, 2018; ISBN 978-1-78923-265-3.
4. Góral, D.; Kluza, F. Heat transfer coefficient in impingement fluidization freezing of vegetables and its prediction. *Proc. Int. J. Refrig.* **2012**, *35*, 871–879. [CrossRef]
5. Góral, D.; Kluza, F. Cutting test application to general assessment of vegetable texture changes caused by freezing. *J. Food Eng.* **2009**, *95*, 346–351. [CrossRef]
6. Korkerd, K.; Soanuch, C.; Zhou, Z.; Piumsomboon, P.; Chalermsinsuwan, B. Correlation for predicting minimum fluidization velocity with different size distributions and bed inventories at elevated temperature in gas-solid fluidized bed. *Adv. Powder Technol.* **2022**, *33*, 103483. [CrossRef]
7. Yang, W. *Handbook of Fluidization and Fluid-Particle Systems*; Marcel Dekker, Inc.: New York, NY, USA, 2003.
8. Shao, Y.; Li, Z.; Zhong, W.; Bian, Z.; Yu, A. Minimum fluidization velocity of particles with different size distributions at elevated pressures and temperatures. *Chem. Eng. Sci.* **2020**, *216*, 115555. [CrossRef]
9. Rezaei, H.; Sokhansanj, S.; Lim, C.J. Minimum fluidization velocity of ground chip and ground pellet particles of woody biomass. *Chem. Eng. Process. Process Intensif.* **2018**, *124*, 222–234. [CrossRef]
10. Li, Y.; Zhou, C.; Lv, G.; Ren, Y.; Zhao, Y.; Liu, Q.; Rao, Z.; Dong, L. Prediction of minimum fluidization velocity in pulsed gas–solid fluidized bed. *Chem. Eng. J.* **2021**, *417*, 127965. [CrossRef]

11. Zhou, Z.Y.; Pinson, D.; Zou, R.P.; Yu, A.B. Discrete particle simulation of gas fluidization of ellipsoidal particles. *Chem. Eng. Sci.* **2011**, *66*, 6128–6145. [CrossRef]
12. Ergun, S. Fluid flow through packed columns. *Chem. Eng. Prog.* **1952**, *48*, 89–94.
13. Senadeera, W.; Bhandari, B.R.; Young, G.; Wijesinghe, B. Influence of shapes of selected vegetable materials on drying kinetics during fluidized bed drying. *J. Food Eng.* **2003**, *58*, 277–283. [CrossRef]
14. Thompson, T.L.; Clark, N.N. A holistic approach to particle drag prediction. *Powder Technol.* **1991**, *67*, 57–66. [CrossRef]
15. Khan, S.A.; Taj, F.; Habib, S.; Shawl, F.; Hussain Dar, A.; Dwivedi, M. CFD Analysis of Drying of Cereal, Fruits, and Vegetables. In *Advanced Computational Techniques for Heat and Mass Transfer in Food Processing*; CRC Press: Boca Raton, FL, USA, 2022; pp. 235–246. ISBN 9781003159520.
16. Smith, P.G. Applications of Fluidization to Food Processing. *Int. J. Food Sci. Technol.* **2009**, *44*, 1867. [CrossRef]
17. Chhabra, R.P.; Agarwal, L.; Sinha, N.K. Drag on non-spherical particles: An evaluation of available methods. *Powder Technol.* **1999**, *101*, 288–295. [CrossRef]
18. Shilton, N.C.; Niranjan, K. Fluidization and its applications to food processing. *Food Struct.* **1993**, *12*, 199–215.
19. Figura, L.O.; Teixeira, A.A. *Food Physics: Physical Properties—Measurement and Applications*; Springer: Berlin/Heidelberg, Germany, 2007; pp. 1–550. [CrossRef]
20. AOAC. AOAC: Official Methods of Analysis, 1980. *Assoc. Off. Agric. Chem. Wash. DC* **1980**, *552*, 517.
21. Frączek, J.; Reguła, T. Methodological aspects of measuring the aerodynamic properties of particles of plant materials. *Acta Agrophys.* **2012**, *19*, 515–525.
22. Gabitto, J.; Tsouris, C. Drag coefficient and settling velocity for particles of cylindrical shape. *Powder Technol.* **2008**, *183*, 314–322. [CrossRef]
23. Mohsenin, N.N. *Physical Properties of Plant and Animal Materials: V. 1: Physical Characteristics and Mechanical Properties*; Routledge: New York, NY, USA, 2020.
24. Kunii, D.; Levenspiel, O. *Fluidization Engineering*, 2nd ed.; John Wiley & Sons, Ltd.: New York, NY, USA, 1991.
25. Polat, S. Heat and mass transfer in impingement drying. *Dry. Technol.* **1993**, *11*, 1147–1176. [CrossRef]